

## ● Review

# Deformation, Phase Transformation and Recrystallization in the Shear Bands Induced by High-Strain Rate Loading in Titanium and Its Alloys

Yongbo XU<sup>1)†</sup>, Yilong BAI<sup>2)</sup> and M.A.Meyers<sup>3)</sup>

1) Shenyang National Laboratory for Materials Science, Institute of Metal Research, Chinese Academy of Sciences, Shenyang 110016, China

2) Laboratory for Non-linear Mechanics of Continuous Media, Institute of Mechanics, Chinese Academy of Sciences, Beijing 100080, China

3) Department of Mechanical and Aerospace Engineering, University of California, San Diego, La Jolla, CA 920930-0411, USA

[Manuscript received February 16, 2006, in revised form April 24, 2006]

$\alpha$ -titanium and its alloys with a dual-phase structure ( $\alpha+\beta$ ) were deformed dynamically under strain rate of about  $10^4 \text{ s}^{-1}$ . The formation and microstructural evolution of the localized shear bands were characterized by scanning electron microscopy (SEM) and transmission electron microscopy (TEM). The results reveal that both the strain and strain rate should be considered simultaneously as the mechanical conditions for shear band formation, and twinning is an important mode of deformation. Both experimental and calculation show that the materials within the bands underwent a superhigh strain rate ( $9 \times 10^5 \text{ s}^{-1}$ ) deformation, which is two magnitudes of that of average strain rate required for shear band formation; the dislocations in the bands can be constricted and developed into cell structures; the phase transformation from  $\alpha$  to  $\alpha_2$  within the bands was observed, and the transformation products ( $\alpha_2$ ) had a certain crystallographic orientation relationship with their parent; the equiaxed grains with an average size of  $10 \text{ }\mu\text{m}$  in diameter observed within the bands are proposed to be the results of recrystallization.

**KEY WORDS:** Localized shear bands; Microstructure; Dislocations; Twinning; Phase transformation; Recrystallization

## 1. Introduction

Metals and alloys may be deformed plastically by dislocation glide, twinning or transformation. Shear deformation localization, shear instability and adiabatic shear which manifest in adiabatic shear bands are known to occur in many extreme inhomogeneous deformation processes in such diverse areas as ballistic impact, explosive fragmentation, high-speed shaping and forming, machining, high velocity fabrication wear in a diverse of materials, including metals, alloys, composites and even engineering plastics. The initiation of the shear localization is a critical event, which can be triggered by either external geometric factors, resulting from stress and strain concentration, or material internal microstructural factors, arising from the structural softening by some mechanisms in the specimens tested. The occurrence of shear instability is an important mode of deformation, and once it occurs, the materials always appear to be failure with low ductility and toughness. Needleman<sup>[1]</sup> has mentioned that “now everybody loves a localization problem, and such localizations are of significance as a precursor to fracture as a mechanism of plastic deformation”, and Rogers<sup>[2]</sup> has also pointed out that “the localization is always catastrophic”. Because of its technological importance, localization poses an in-

teresting challenge to scientists in mechanics, materials and even physics, and much attention has been paid on the aspects of both mechanics and materials during the past thirty years. Theoretically, mechanicians have focused their efforts on the constitutive analysis. They have intended to determine the critical conditions for the plastic flow instability<sup>[3~9]</sup> and a variety of constitutive models have been proposed to describe localized shear. Experimentally however, the materials scientists have concerned the effect of localized shear deformation on the mechanical behavior of materials. They want to understand how the microstructural parameters influence the occurrence of shear instability, and then design a material with higher resistance to shear band formation, delay or even control the proliferation of the shear localization, and hence get better performance. A number of reviews<sup>[2,10,11]</sup> and articles<sup>[12~18]</sup> are available.

Titanium and its alloys are very susceptible to localized shear deformation which dominates deformation behavior of the alloys under high-strain rate loading. Therefore, localized shear deformation of titanium and its alloys has been investigated extensively in recent years<sup>[19~36]</sup>. Winter<sup>[19]</sup> has studied the shear bands of Ti-6Al-4V alloy produced during impact loading. He found that the shear band was composed of the fine grains in which the microhardness was higher than that of regions outside the band, and the spherical cavities distributed along the shear bands. Hence he considered that the material in the

† Prof., to whom correspondence should be addressed,

E-mail: ybxu@imr.ac.cn.

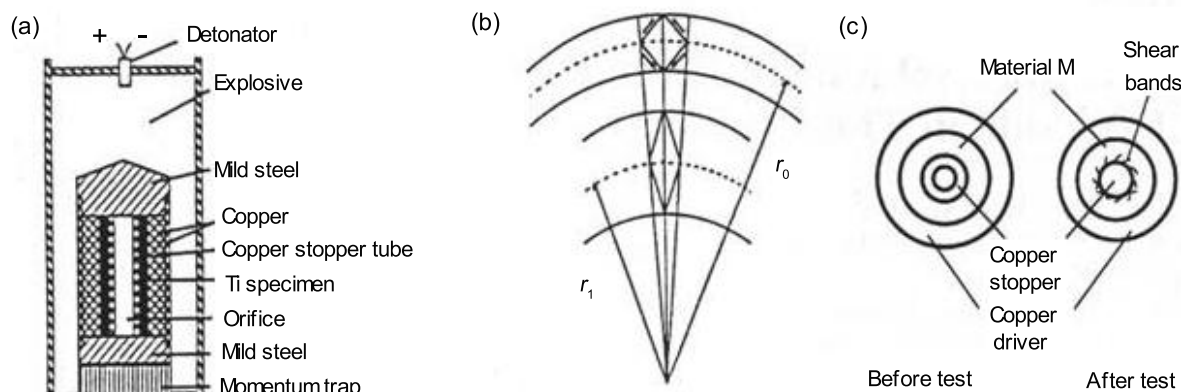


**Fig.1** Experimental configuration for collapse of thick-walled cylinder (a), pure shear deformation of an element as tube collapses (b), and cross-sections of the shear bands after explosion (c)

band was very hot (possibly molten) and had then recrystallized. Timothy and Hutchings<sup>[21,22]</sup> have observed the white-etching band, resulting from ballistic impact in Ti-6Al-4V with different microstructures, and found that the well-developed bands consisted of zones of intense shearing distortion of the original microstructure, modified by the effects of elevated temperature. They concluded that there was no clear evidence in this alloy to suggest that the shear bands had undergone a martensitic phase transformation. Me-Bar and Shechtman<sup>[23]</sup> have reported that the high temperature generated in the band in Ti-6Al-4V ballistic targets could cause a transformation from the  $\alpha$  to  $\beta$ -phases, and in some instances might lead to melting. Bayoumi and Xie<sup>[27]</sup> have reported that a non-diffusion phase transformation which led to the loss of the  $\beta$ -structure took place in the process of shear band formation during machining of the Ti-6Al-4V alloy. Based on either the appearance of the shear band or the measured temperature rise, Liao and Duffy<sup>[28]</sup> have suggested that the material within the bands in Ti-6Al-4V had undergone a phase transformation. Recently, Deepak *et al.*<sup>[32]</sup> have reported an investigation of shear band growth and microstructural evolution of  $\alpha$ -titanium using transmission electron microscopy (TEM) observation, and they found the following results: planar dislocation motion and twinning, and grouping of dislocations into cells as well as development of equiaxed grains occur in the band. Their observations are similar to those which were obtained by Meyers *et al.*<sup>[33]</sup> in the same material of  $\alpha$ -titanium. Li *et al.*<sup>[34]</sup> have studied formation of the shear bands in Ti-6Al-4V target which was impacted by GCr15 steel balls at a speed of 1.5 km/s. They found that two-types of adiabatic shear bands: deformed- and white-etching bands formed near the craters. They proposed that the former formed at an early stage of localization, and then the latter transformed into the white-etching band with increasing the strain.

This paper presents an extensive overview and investigation of the microstructural evolution within the localized shear bands, including  $\alpha'$ -phase transformation, recovery and recrystallization, twinning and high-order twinning as well as superhigh strain rate deformation characteristics in the bands of the titanium

and its alloys.

## 2. Experimental Techniques and Materials

$\alpha$ -titanium and its titanium alloys with a dual-phase structure ( $\alpha+\beta$ ) of Ti-6Al-4V and Ti-4.0Al-2.0Zr-1.0Mo-0.8Nd-0.25Sn were selected to study localized shear behavior induced during deformation dynamically. The alloys were heat treated, and the resulting microstructure is composed of equiaxed grains.

### 2.1 Shear band generation

The localized shear bands were generated by two methods: (1) The cylinder-impact specimen with a diameter of 4.0 mm and height of 4.0 mm, using a split Hopkinson pressure bar (SHPB) in a compression mode to generate large shear strain in the direction of about  $45^\circ$  to the compression direction. (2) The explosive collapse of a thick-walled cylinder under controlled conditions which was developed by Nesterenko and Bondar<sup>[37]</sup>. The specimen is sandwiched between a copper driver tube and a copper stopper tube and is collapsed inwards during the test. The internal diameters of the inner copper tube were selected to produce prescribed and controlled final strains. In some special cases, a central steel rod was also used. The explosive is axisymmetrically placed around the specimen. The detonation is initiated on the top. The expansion of the detonation products exerts a uniform pressure on the cylindrical specimen and drives the specimen to collapse inward (Fig.1(a)). The detonation velocity of the selected explosive is approximately 4000 m/s and its density is 1 g/cm<sup>3</sup>. The velocity of the inner wall of the tube was determined by an electromagnetic gage, and the initial velocity of collapse of the inner tube was found by Xue *et al.*<sup>[18]</sup> to be approximately 200 m/s. The stress state generated within the collapsing cylinder before localized shear is one of pure shear as shown in Fig.1(b). Selected dimensions of copper tubes sandwiched in the sample control the collapse of thick-walled cylinder specimen. Figure 1(c) shows schematically cross-sections of the localized shear bands produced during explosion. They have spiral trajectories and initiate at the internal surface of the cylinder. The strain rate imparted is in the order of  $10^4$  s<sup>-1</sup>. The unstable deformation, which is initially homogeneous, gives rise to

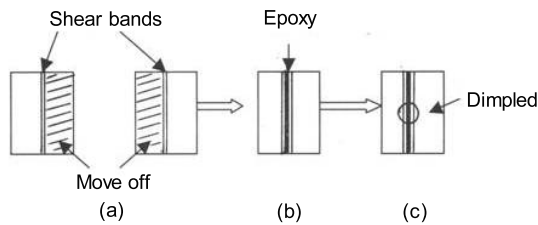


**Fig.2** Cross-section and butt method for preparing TEM sample: (a) cross section, (b) and (c) butt

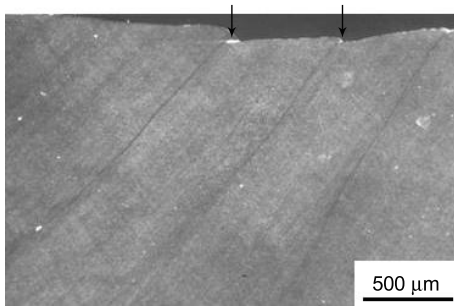


**Fig.3** FESEM micrograph of the cross-section of a thick-walled cylinder specimen showing that a number of localized shear bands initiate at the internal surface (indicated by arrows), and propagate outwards

shear bands along the internal surface. These bands grow outward to the thick-walled cylinder.

## 2.2 Microstructure characterization

Very thin region of shear deformation localization makes the microscopic examination difficult, particularly in making thin-foil specimen for TEM examination, because the perforation produced by known ordinary methods such as double jet polishing and ion-milling, does not just correspond to the region of the shear band. Therefore, “cross-section and butt” method was used in some special cases to prepare thin-foils for TEM observations. First, the matrix material on one side of the band was moved off (Fig.2(a)), and then, two or three bands were butted and glued face to face (Fig.2(b)) till the epoxy was then cured. After then, the specimens were mechanically ground and dimpled to a thickness of less than 20  $\mu\text{m}$  as shown in Fig.2(c). The microstructure and its evolution characteristics within the shear bands were examined by field emission scanning electron microscopy (FESEM) and TEM.

## 3. Results and Discussion

### 3.1 Topography and distribution of the shear bands

The collapse of thick-walled cylinder specimen generates in a plane strain condition, and the stress state can be considered as a superposition of a hydrostatic pressure and a pure shear stress due to the axisymmetrical geometry and loading. While the radial stress is zero at the internal surface, the tangential stress is maximum. The shear stress is highest at the internal surface, and this is where shear localization starts. Figure 3 is typical FESEM micrograph of the cross-section of a thick-walled cylinder

specimen of Ti-6Al-4V alloy which was subjected to explosive testing. It can be found that a number of localized shear bands initiate at the internal surface of the thick-walled cylinder, and propagate outwards, leaving the big steps behind at the internal surface indicated by arrows, and some of them appear to be cracking along the length of the bands because of highly localized shear strain. The height of the step in the inner surface (Fig.3) provides a displacement. The displacement, divided by the thickness of the bands, gives the shear strain. Routinely, shear strain as high as 100 was achieved. The angle between the shear and radial directions is around  $45^\circ$  which is the plane of maximum shear stress (strain). It is seen clearly that the distribution of the shear band pattern appears to be regular (Fig.3). This characteristic spacing and a periodical distribution of the bands are a function of material parameters<sup>[18]</sup>. Figure 4 shows a long and straight shear band occurred when the cylindrical specimen was subjected to an explosive loading, and Fig.5 shows the initiation and coalescence of the voids within the bands. From Figs.3, 4 and 5, several features should be mentioned. First, the thickness of the band is not uniform, but changes between 10~30  $\mu\text{m}$ , indicating that the shear strains would correspondingly change. Second, the voids generated within the band appear to be elliptical, and some of them are connected under the combined action of the shear and normal stresses. Obviously, the temperature rise and high strain in the bands promote the nucleation and connection of the voids, leading to final fracture of materials with low toughness and low ductile along the bands. Third, severely deformed and destroyed structures in the band can be seen clearly when the comparison of the microstructures is made between inside and outside the band. In addition to these, another important feature of the bands found in the exploding cylinder geometry is that the end of the bands is not sharp, but divergent. This referred to as bifurcation, is geometrically necessary due to the spiral trajectory of the bands, starting in the internal surface<sup>[18]</sup>.

### 3.2 Deformed and “transformed” bands

The localized shear bands can be classified as either deformed bands or “transformed” bands on the basis of their appearance in metallographic section<sup>[38]</sup>. The “transformed” bands are often referred to as white-etching bands or white shear bands in steels, and have been received much attention because once the phase transformation occurs within the bands it suggests that phase transformation temperature is reached in the narrow band of material, supporting the thermo-plastic instability theory of shear localization. In addition to steels, the white-etching bands have been reported extensively also in titanium and titanium alloys<sup>[21,22,30]</sup>. Figure 6 shows two types of shear bands in a titanium alloy subjected to dynamic impact compression bands produced in Ti-4.0Al-2.0Zr-1.0Mo-0.8Nd-0.25Sn alloy under high-strain rate impact compression. The evidence for occurrence of phase transformation in the bands in steels seems to rise from the white in a natal etch, a well-defined width, distinct boundaries between the band and the matrix, and also very high hardness. Trent<sup>[39]</sup> made the earliest observation of the white-etching

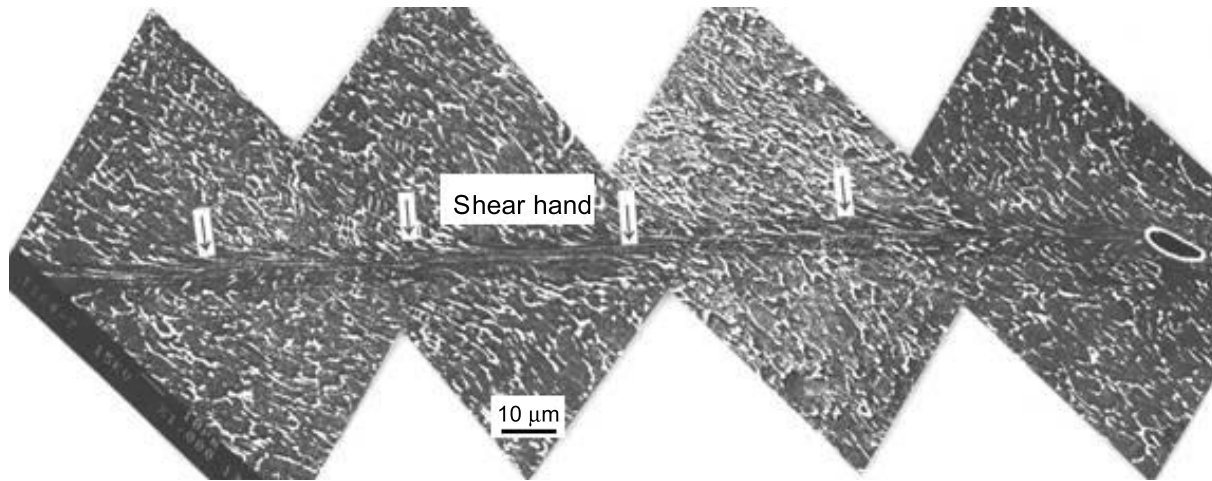


**Fig.4** SEM montages, showing a long and straight shear deformation band produced during explosion

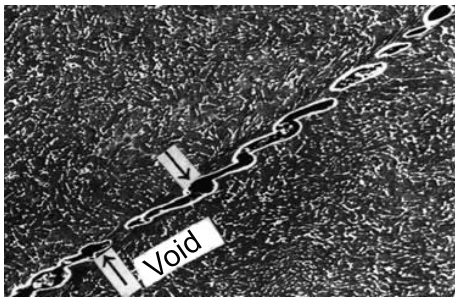


**Fig.5** Void initiation and coalescence produced during explosion within the bands of Ti-6Al-4V alloy

bands generated in steel, and he found these bands appeared to be white or slightly yellow on the sheared surface. He assumed that this must be retained austenite. Zener and Hollomon<sup>[38]</sup> have reported that the white-etching bands were caused by a rapid quenching from the high temperature, and they suggested that the strain rates in their punching test may reach  $2.0 \times 10^3 \text{ s}^{-1}$  and temperature in the bands may rise as high as  $1000^\circ\text{C}$ , and hardness of the shear bands led Zener and Hollomon to postulate that the bands were untempered martensite. Andrew *et al.*<sup>[40]</sup> have studied the white lines in Ni-Cr steel and suggested that both martensite and austenite may form, and they considered that the austenite may be retained. However, Scott *et al.*<sup>[41]</sup> have reported that the white-etching bands could not show the tempering characteristics of conventional martensite even when heated to temperatures above normal tempering temperatures. Timothy and Hutchings<sup>[21]</sup> have studied the shear bands in Ti-6Al-4V alloy, and they have not found the martensitic phase transformation to occur in this alloy. As regards the temperature rise in the bands, a number of authors proposed that the temperature rise during shear localization may reach several hundred degrees above that of the surrounding matrix. This is usually inferred indirectly from metallurgical evidence, and the shear band is then proposed to be rapidly cooled by the surrounding bulk material when plastic deformation ceases, and cooling rates as high as  $10^7 \text{ K}\cdot\text{s}^{-1}$  have

been calculated<sup>[23]</sup>. However, some authors have been made directly measurements<sup>[40~47]</sup> and they found that the highest temperature in the band region was in the range of  $440\sim 550^\circ\text{C}$  for Ti-6Al-4V<sup>[40]</sup>,  $450^\circ\text{C}$  for AISI 1018 cold rolled steel and AISI 1020 steel<sup>[44,45]</sup>,  $590^\circ\text{C}$  for HY-100 steel<sup>[43]</sup>, and  $460^\circ\text{C}$  for AISI 4340 steel<sup>[46,47]</sup>, respectively. These measurements indicate that the material within the shear band had not undergone a phase transformation either in steels or in titanium alloys. A number of investigations show that there are many indications that the white-etching shear bands may have different structures in different materials and even that the structures may be different in parts of the bands<sup>[2]</sup>, and whether deformed or transformed-bands, their formation corresponds to different deformation stages, and the deformed band forms at earlier stage of localization, and as deformation proceeds, the white-etching band develops within the deformed bands<sup>[17,22]</sup>. Their presence is generally indicated by the different etching response in a narrow band of material in metallographic cross-sections. The difference in structure orientation in the white-etching bands is too small to be recognized by ordinary optical microscopy and SEM. In other words, both the ordinary light and secondary electron wave could not be able to “see” the substructure difference in orientation in the bands. So it is reasonable to propose that the white-etching is unlikely to be the occurrence of phase transformation in the bands. Recent investigations have shown however, that the phase transformation is surely to occur in the deformed-type bands, which will be described in the next section.

### 3.3 Phase transformation in the shear bands

Recent investigations have revealed that the  $\alpha'$ -martensitic phase transformation occurs in the shear bands in stainless steel<sup>[17]</sup> and Fe-Cr-Ni single crystal<sup>[48]</sup>, and this kind of phenomenon has also been observed in the shear bands in Ti-6Al-4V. Figure 7 gives a set of TEM montage, showing that  $\alpha_2$  phases occur in the band of the alloy. Figure 7(a) is bright-field image taken from the primary- $\alpha$  grains in the band, and Fig.7(b) is its combined electron diffraction pattern. Fig.7(c) and (d) are the dark-field images which were obtained by using strong diffraction

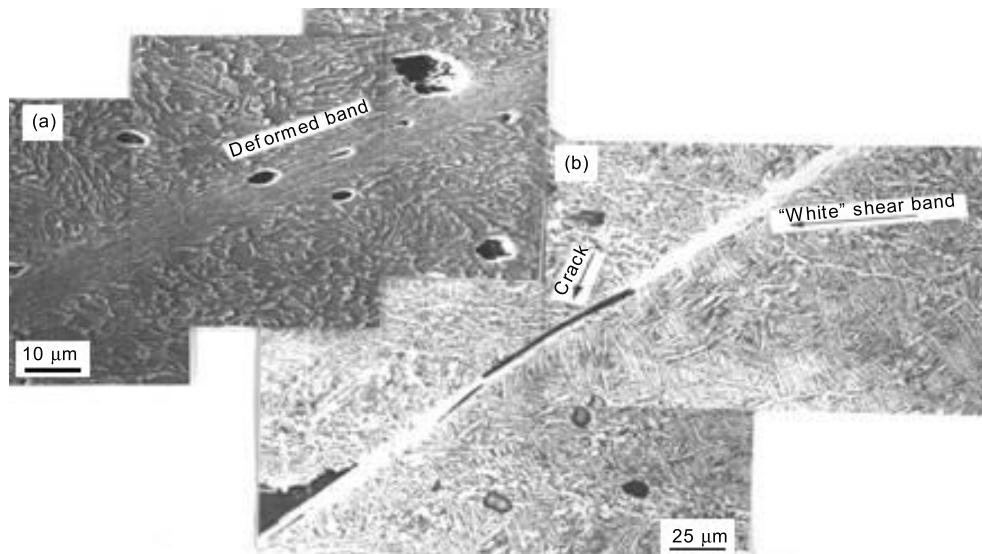


**Fig.6** Deformed (a) and white-etching band (b) observed

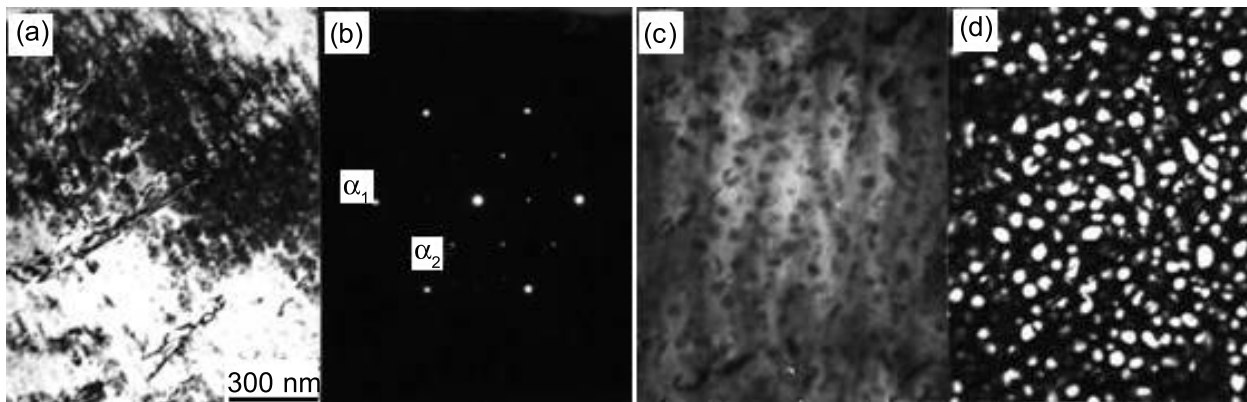


**Fig.7** TEM montage, showing bright-field of the high-strain rate deformation structure in Ti-6Al-4V alloy (a), its [0001] zone axis diffraction pattern (b), and dark-field images obtained by using strong diffraction spots  $\{2200\}_{\alpha}$  marked by  $\alpha$  (c) and weak super-lattice reflection  $\{1100\}_{\alpha_2}$  marked by  $\alpha$  (d), respectively

( $\alpha$ ) and super lattice reflection ( $\alpha_2$ ) spots, respectively. According to the analysis of electron diffraction and dark-field image, it is confirmed that the  $\alpha_2$ -phases ( $\text{Ti}_3\text{Al}$ ) are proposed to transform from the  $\alpha$ -matrix, and  $z$ -axis of both the  $\alpha$ -phases and  $\alpha_2$ -phases are parallel, and these two phases are completely coherent. This kind of transformation is, to the authors' knowledge, proposed to be the first observation within the shear bands in this alloy subjected to explosive loading. Me-Bar and Shechtman<sup>[23]</sup> have studied the shear bands induced during ballistic impacting in Ti-6Al-4V alloy, and suggested that the temperature generated in the bands could cause a transformation from the  $\alpha$  to  $\beta$ -phase. Bayoumi and Xie<sup>[27]</sup> suggested that a non-diffusion phase transformation which led to the loss of the  $\beta$ -phases, might take place in the process of shear band formation in Ti-6Al-4V alloy. In regard to  $\alpha \rightarrow \alpha_2$  ( $\text{Ti}_3\text{Al}$ ) transformation in the titanium alloys, Mendiratta *et al.*<sup>[49]</sup> have reported that the  $\alpha_2$  ( $\text{Ti}_3\text{Al}$ ) precipitation may occur in Ti-6Al-2Sn-4Zr-2Mo alloy during creep. Li and Wan<sup>[50]</sup> have investigated  $\text{Ti}_3X$  (where  $X=\text{Al}$ , V, and Zr) phase formation in a titanium alloy during heat treatment, and they found that when the

content of  $X$  in the alloy reaches a critical solution degree, the long-region ordered phase ( $\text{Ti}_3X$ ) with super lattice structure starts to occur in  $\alpha$ -Ti, and they suggested that this is a process of transformation from disordered  $\alpha$  to ordered  $\alpha_2$ . The morphology of the  $\text{Ti}_3X$  phases they observed is spheroid with 20 nm in diameter which is completely similar to the results at present investigation. However, the transformation from  $\alpha$  to  $\alpha_2$  induced by high-strain rate in Ti-6Al-4V alloy has not been reported so far, and further studies of the transformation mechanism are still needed.

### 3.4 Mechanical conditions for shear band formation

The criterion for shear band formation has been one of the most interesting projects, and a number of approaches have been focused on the theoretical treatments, consisting of the combination of a mechanical instability analysis with a thermal model for over two decades. A number of researchers have proposed that once a critical strain corresponding to a macroscopic maximum load on a stress-strain curve has been achieved, the shear bands form<sup>[3~9]</sup>. Recht<sup>[3]</sup> however, concluded that a critical strain rate was

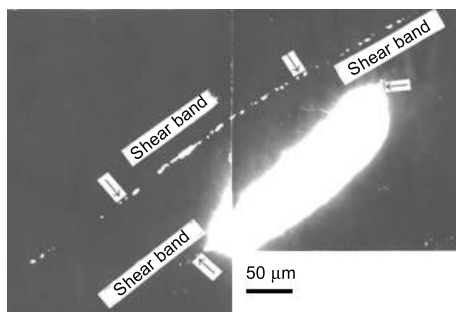


**Fig.8** TEM image, showing two parallel shear bands (indicated by arrows) produced during explosion

required for production of catastrophic shear based on his result of titanium which was subjected to the machining dynamically. Zurek<sup>[51]</sup> has studied the white-etching bands in 4340 steel, and reported that the average strain of 0.5 and the associated average strain rate of  $1.8 \times 10^4 \text{ s}^{-1}$  were sufficient to induce an adiabatic shear instability. Rogers<sup>[2]</sup> has pointed out that “large strain can be achieved quasi-statically in steel without transformed band formation; hence, provide that a minimum strain achieved, there must exist a strain rate above which the removal of heat from the region of deformation is sufficiently limited that the temperature can rise above that needed for transformation to occur—a critical strain rate”. All these imply that both strain and strain rate should be required for shear band formation. Unfortunately, few experimental data are available that can be directly compared with these analyses to verify and guide model development of shear banding. Recent investigations show that in addition to strain, strain rate should be considered simultaneously as the mechanical conditions for shear band formation. An example is the localization process produced during high-speed impact loading in Ti-4.0Al-2.0Zr-1.0Mo-0.8Nd alloy and shows that when the strain rate reaches  $1.75 \times 10^3 \text{ s}^{-1}$ , corresponding to a strain of 16, the deformed shear bands appear at first as shown in Fig.6(a), and as deformation proceeds, the width of the band becomes gradually narrower. When the strain rate is approximately  $2.0 \times 10^3 \text{ s}^{-1}$ , corresponding to strain of 20, the white shear bands occur as a result of the further development of the deformed bands as shown in

Fig.6(b)<sup>[52]</sup>. This result confirms further the similar observation in the Al-Li alloys<sup>[53]</sup> and is verified by recent observations<sup>[36,54,55]</sup>, and also supports experimentally the theoretical prediction<sup>[5]</sup>.

### 3.5 Slip and twinning

Slip and twinning are two kinds of essential modes of deformation in materials, and they both are competing processes. It is generally expected that the twinning should become active and important mechanism of deformation at low temperature and high strain rate. In particular for the materials with hcp structure, the twinning may be the dominant mechanism of deformation. The image shown in Fig.8 is the low-magnification of the TEM bright-field, displaying two parallel localized shear bands (indicated by arrows) generated in Ti-6Al-4V alloy which is subjected to explosive collapsed loading at room temperature, and all observations of the microstructure induced by the dynamic loading are performed on these two bands. Figure 9 shows typical substructures for Ti-6Al-4V in the central area along the shear band. Analysis shows that the dislocations with Burgers vector of  $[0001]$  determined under two-beam condition developed the tangled dislocations (Fig.9(a)), and the dislocations with Burgers vector  $1/3[11\bar{2}0]$  were constricted and organized into well developed cell-walls (Fig.9(b)), suggesting that the recovery processes are active in these areas. These observations clearly indicate that the microstructure varies across the shear band, implying that the strain in the band appears to be also varied from point to point. Figure 10 is a set of TEM micro montage, showing the highly deformed structure of the shear bands. Figure 10(a) is a bright-field image of the multi-twin with high dense dislocation. Figure 10(c) is its electron diffraction. Figure 10(b) is the dark-field images of the Fig.10(a). They were obtained by  $T_1$  and  $T_2$  in Fig.10(b), respectively. The similar observation is shown in Fig.11, from which it can be seen clearly that the thin micro-twin segments may produce within the twins (indicated by arrows), and this kind of twinning is proposed to be a continued and multiplied processes dynamically. These microtwin segments are generally very thin with about several atom layers in thickness<sup>[17]</sup>. Trace analysis shows that twinning is mainly on  $\{10\bar{1}2\}$  and  $\{11\bar{2}1\}$  planes.

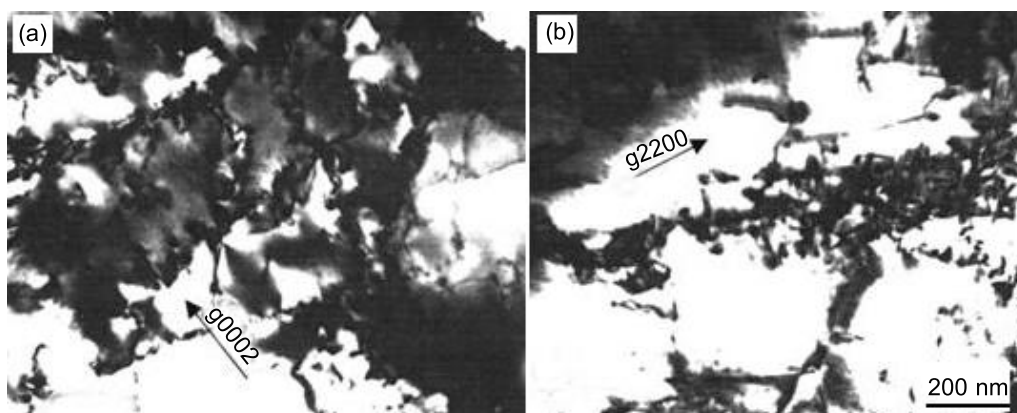


**Fig.9** Bright-field image of the dislocations obtained under two-beam condition. The reflection  $g=0002$  is shown (a) and dislocations with Burgers vector of  $1/3[11\bar{2}0]$  (b) are constricted to form the cell structures. The reflection  $g=2200$  is shown

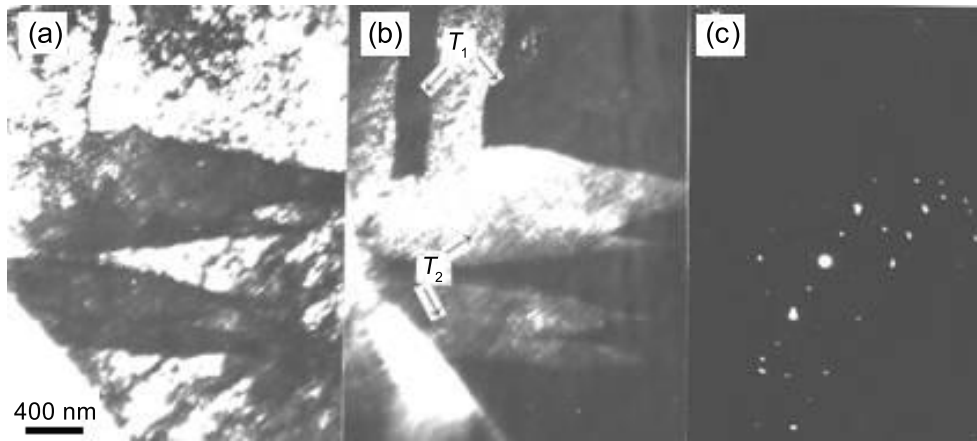


**Fig.10** High-order twins with high density dislocation in a specimen subjected to explosive collapsed loading: TEM bright-field (a) and its electron diffraction pattern (c), and dark-field image (b) obtained by a weak diffraction spot in (c)

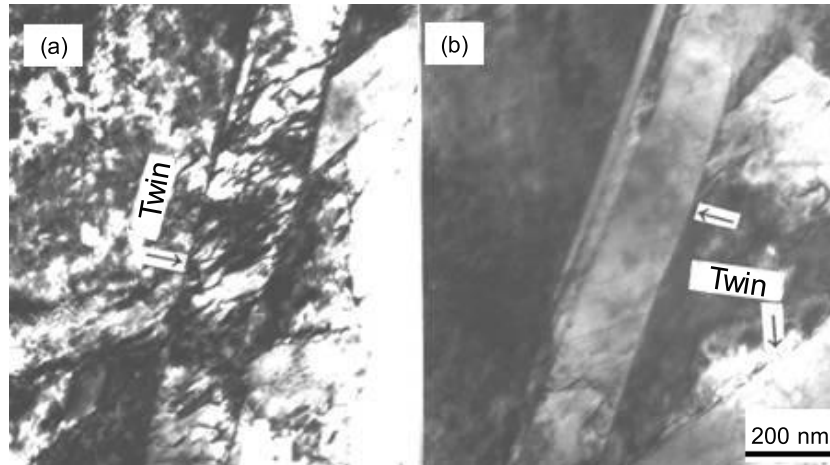


**Fig.11** High-order twins and high density of dislocations viewed end-on in both inside (a) and outside (b) the twins

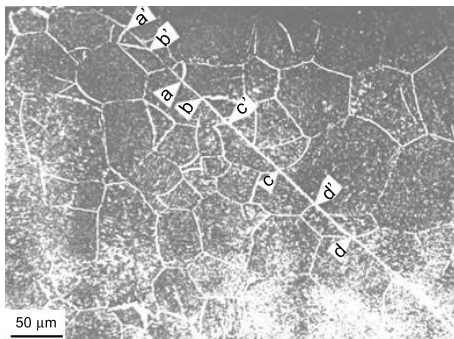


**Fig.12** Shear band in  $\alpha$ -Ti developed during dynamic compression. The grains were sheared by shearing deformation

### 3.6 Superhigh strain rate deformation within the band

It is well known that once localized shear deformation has commenced, steep strain and strain rate as well as temperature rise will appear in the shear bands. Li<sup>[56]</sup> has made an interesting observation and calculation of strain rate within white-band in  $\alpha$ -Ti as

shown in Fig.12, where it can be seen that both sides of the band were made a relative displacement, for example, the displacements from  $a$  to  $a'$ ,  $b$  to  $b'$ ,  $c$  to  $c'$  and  $d'$  to  $d$  occur during localization. From these, the average shear strain was measured to be 5.2, and the width of the shear band was 12  $\mu\text{m}$ . According to the equation proposed by Dodd and Bai<sup>[57]</sup>, the half-width of the shear band is expressed as follows:

$$\delta = \sqrt{\frac{\lambda \theta_*}{\tau_* \dot{\gamma}_*}} \quad (1)$$

the temperature rise within the bands obtained by assuming that 90% of deformation work is converted into heat:

$$\theta_* = \frac{0.9 \tau_* \gamma_*}{\rho \cdot c} \quad (2)$$

The time required for shear band formation can be obtained by the following equation from Eq.(1) with Eq.(2):

$$t = \gamma_* / \dot{\gamma}_* = \frac{\rho c}{0.9 \lambda} \delta^2 \quad (3)$$



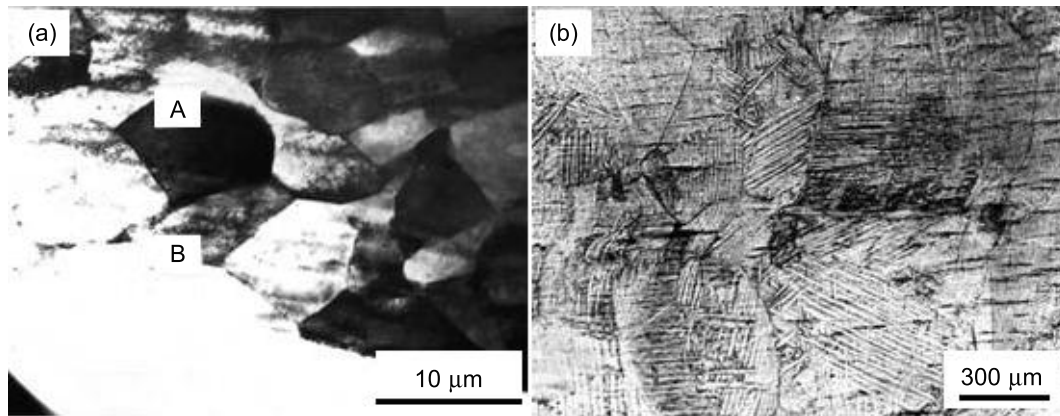


**Fig.13** Equiaxed and distortion-free grains observed within the shear band (left) and very large grains (right) outside the shear band in Ti-6Al-4V

where  $\tau_*$ ,  $\gamma_*$ ,  $\dot{\gamma}_*$  are the shear stress, shear strain, and strain rate,  $\theta_*$  is the temperature rise in the band,  $\lambda$  is the coefficient of the heat conduction,  $\rho$  is the material density and  $c$  is the heat capacity. The parameters used in Eq.(3) are:  $\rho=4.5 \text{ g}\cdot\text{cm}^{-3}$ ,  $c=0.473 \text{ J}\cdot\text{g}^{-1}\cdot\text{K}^{-1}$ ,  $\lambda=14.63 \text{ W}\cdot\text{m}^{-1}\cdot\text{K}^{-1}$ , for  $\alpha$ -Ti, and  $t=0.1616\delta^4$ , where the unit of the  $t$  is  $\mu\text{s}$ , and the unit of  $\delta$  is  $\mu\text{m}$ .

From Eq.(3), it is found that the time required for formation of the band is  $5.8 \mu\text{s}$ , and therefore, strain rate that the shear band underwent is  $9\times 10^5 \text{ s}^{-1}$  which is much higher, by two orders of magnitude, than that average strain rate ( $2\times 10^3 \text{ s}^{-1}$ ) required for formation of the shear band, implying that formation of the shear band may company an abrupt increase in strain rate. In other words, the materials within the band underwent a super-high-strain rate deformation. This is confirmed by Xu *et al.*<sup>[53]</sup> in the investigation of Al-Li alloy. They have determined strain rate within the band, and found that the local strain in band is 10.0, and the time for band formation is equal to about  $100 \mu\text{s}$ , and then the strain rate within the band is about  $10\times 10^5 \text{ s}^{-1}$  which is much higher than that of the average strain rate ( $2.6\times 10^3 \text{ s}^{-1}$ ) required for formation of the bands. Giovanola<sup>[58]</sup> measured directly shear strain rate in the shear band as a function of time in VAR 4340 steel by using a high-speed photography technique, and found that shear localization occurs in two sequential stages, and during the first localization, the strain rate ( $10^4 \text{ s}^{-1}$ ) jumps by more than an order of magnitude to values larger than  $10^5 \text{ s}^{-1}$ , then approaching  $1.4\times 10^6 \text{ s}^{-1}$  during second localization. Such very high strain and strain rate produced during localization in the bands have also reported previously<sup>[59~69]</sup>. A number of investigations show that a polycrystalline material with high strain rate sensitivity will appear to be deformed at a mode of super-plastic flow<sup>[61,62]</sup>. First, the structures in the shear bands are very fine. For example, if recrystallization occurs, the new grain size is lower than  $0.1 \mu\text{m}$ ; second, the temperature in the bands may reach, and even higher than  $0.4T_m$  ( $T_m$  is the melting temperature), all these provide the conditions for super-plastic deformation of the materials in the bands. Ashby and Verrall<sup>[63]</sup> have proposed a constitutive equation to describe super-plastic flow of a

material under high strain rate as follows:

$$\dot{\epsilon} = 98\Omega/kTd^2\{\sigma - 0.72\Gamma/d\}D_v \cdot (1 + \Pi\delta/d \cdot D_B/D_v)$$

where  $\dot{\epsilon}$ : strain rate;  $\Omega$ : atomic volume;  $k$ : Boltzmann's constant;  $T$ : absolute temperature;  $d$ : grain size;  $\sigma$ : tensile stress;  $\Gamma$ : grain boundary free energy;  $D_v$ : bulk diffusion coefficient;  $\delta$ : grain boundary width;  $D_B$ : boundary diffusion coefficient. They suggested that when polycrystalline matter is deformed at temperature above  $0.4T_m$ , one possible mode of super plastic flow is a "diffusion-accommodated flow". Dodd and Bai<sup>[57]</sup> have pointed out that in the process of machining, although the average strain rate may be quite low, the strain rate in these narrow bands of shear may be markedly higher. Murr *et al.*<sup>[64]</sup> have also suggested that "the shearing deformation actually achieved inside an adiabatic shear band is extremely large; with shear strains as large as 10, and the mechanism to achieve this large strain involves dynamic recrystallization (DRX) and superplastic flow by sliding of submicron, equiaxed recrystallized grains".

### 3.7 Recrystallization

Dynamic recrystallization, arising from high-strain rate loading has been documented by some researchers, and observed mainly in steels<sup>[18,66~68]</sup>, and also in copper<sup>[69~71]</sup>, in tantalum<sup>[72,73]</sup>, and other materials<sup>[74]</sup>, but there has been little work reported in titanium alloys so far. Winter<sup>[19]</sup> studied adiabatic shear bands produced during impact loading in Ti-6Al-4V alloy and based on the spherical cavities observed along the bands. He concluded that the material in the band was very hot (possible molten) and had then recrystallized. However, he did not offer any data and pictures about recrystallization that occur in the bands. Recent investigations show that recrystallization occurs in Ti-6Al-4V alloy. Figure 13 is a set of TEM bright-field images taken from the shear band, showing the equiaxed and distortion-free grains (Fig.13(a)). For comparison, the large grains with an average size of about  $10 \mu\text{m}$  outside the bands are also shown in Fig.13(b). These grains within the band are much smaller than those outside the bands. Electron diffraction analysis indicates that these grains



have low-angle boundaries. For example, the orientation of the grain A is [001] as shown in Fig.13(a), and its contrast is quite different from that of the adjacent grain B at this moment. However, only a rotation of  $1^\circ$  is performed around  $z$ -axis in microscope, the orientation of the grain B is also brought to be [001] (Fig.13(a)), indicating that the angle between both grains of A and B is about  $1^\circ$ . The same operations are also performed on the other grains in the field, and the results show that all boundaries of the grains shown in Fig.13(a) are of low-angles. These equiaxed and distortion-free grains observed within the bands are proposed to be produced by dynamic recrystallization that occurs during explosion, and it was attributed to a rotational recrystallization mechanism<sup>[17]</sup>.

#### 4. Conclusions

(1) Localized shear bands initiate at the internal surface of the Ti-6Al-4V alloy specimen and propagate outwards during explosion.

(2) Two-types of the shear bands: deformed- and white-etching bands were observed in the alloy studied. Their formation corresponds to different deformation stages, and the deformed band forms at earlier stage of localization, and as deformation proceeds, the white-etching band develops within the deformed bands.

(3) There is a critical value of strain for occurrence of the shear bands under certain strain rate condition. In other words, strain and strain rate are both requested for shear band formation.

(4) The dislocations produced during explosion may be constricted to form the cell structure with high-dense dislocations.

(5) The twinning is an active and important mode of deformation in this alloy under explosive loading.

(6) Shear band formation may company an abrupt increase in strain rate which is much higher, by two orders of magnitude, than that average strain rate required for production of the shear band. In other words, the materials within the band underwent a super-high-strain rate deformation.

(7) The equiaxed and distortion-free grains observed within the bands are proposed to be the results of dynamic recrystallization.

(8) The  $\alpha \rightarrow \alpha_2$  (Ti<sub>3</sub>Al) transformation was observed during explosion in Ti-6Al-4V alloy, and the transformed products ( $\alpha_2$ -Ti<sub>3</sub>Al) have a certain crystallographic orientation relationship with their parent.

#### Acknowledgement

This research was supported by the National Nature Science Foundation of China (No. 50071064).

#### REFERENCES

- [1] N.Needleman: *Appl. Mech. Rev.*, 1992, **45**, 53.
- [2] H.C.Rogers: *Ann. Rev. Mater. Sci.*, 1979, **9**, 283.
- [3] R.F.Recht: *J. Appl. Mech-T. ASME.*, 1964, **31**, 189.
- [4] R.J.Clifton: *Material Response to Ultra High Loading Rates*, National Materials Advisory Board Committee, Rep. No. NMAB-356, 1980, 129.
- [5] Y.L.Bai: *J. Mech. Phys. Solids*, 1982, **30**, 195.
- [6] T.J.Burns and T.G.Trucano: *Mech. Mater.*, 1982, **1**, 313.
- [7] F.H.Wu and L.B.Freund: *J. Mech. Phys. Solids*, 1984, **32**, 119.
- [8] M.R.Staker: *Acta Metall.*, 1981, **29**, 633.
- [9] S.Nemat-Nasser: *Appl. Mech. Rev.*, 1982, **45**, S19.
- [10] L.E.Murr and E.V.Esquivel: *J. Mater. Sci.*, 2004, **39**, 1153.
- [11] M.A.Meyers: in *Mechanics and Materials-Fundamentals and Linkages*, eds. by Marc Andre Meyers, Ronald W.Armstrong and Helmut O.K.Kirchner, John Wiley Sons, 1999.
- [12] H.A.Grebe and H-R.Pak: *Acta Metall. Mater.*, 1985, **16A**, 711.
- [13] C.L.Wittman M.A.Meyers and H-R.Pak: *Metall. Trans.*, 1990, **21A**, 707.
- [14] M.A.Meyers and C.L.Wittman: *Metall. Trans.*, 1990, **21A**, 3193.
- [15] Y.L.Bai, Q.Xue, Y.B.Xu and L.T.Shen: *Mech. Mater.*, 1994, **17**, 155.
- [16] Y.B.Xu, Y.L.Bai, Q.Xue and L.T.Shen: *Acta Mater.*, 1996, **44**, 1917.
- [17] M.A.Meyers, Y.B.Xu, Q.Xue, M.T.Perez-Prado and T.R.McNelly: *Acta Mater.*, 2003, **51**, 1307.
- [18] Q.Xue, M.A.Meyers and V.F.Nesterenko: *Acta Mater.*, 2002, **50**, 575.
- [19] R.E.Winter: *Phil. Mag.*, 1975, **31**, 765.
- [20] R.L.Woodward: *Metall. Mater. Trans.*, 1979, **10A**, 569.
- [21] S.R.Timothy and I.M.Hutchings: *Acta Mater.*, 1985, **33**, 667.
- [22] S.R.Timothy: *Acta Mater.*, 1987, **35**, 301.
- [23] Y.Me-Bar and D.Shechtman: *Mater. Sci. Eng.*, 1983, **58A**, 181.
- [24] H.A.Grebe, H-R.Pak and M.A.Meyers: *Metall. Mater. Trans.*, 1985, **16A**, 761.
- [25] A.R.Shahan and A.K.Taheri: *Mater. Design*, 1993, **14**, 243.
- [26] J.C.Williams and M.H.Blackborn: *Trans. Am. Soc. Metal.*, 1967, **60**, 373.
- [27] A.E.Bayoumi and J.Q.Xie: *Mater. Sci. Eng.*, 1995, **190A**, 173.
- [28] S.C.Liao and J.Duffy: *J. Mech. Phys. Solids.*, 1998, **46**, 2201.
- [29] A.Molinari, C.Musquar and G.Sutter: *Int. J. Plasticity*, 2002, **18**, 443.
- [30] Q.Li, Y.B.Xu and M.N.Bassim: *Mater. Sci. Eng.*, 2003, **A358**, 128.
- [31] D.G.Lee, Y.G.Kim, D.H.Ham, S.M.Hur and S.Lee: *Mater. Sci. Eng.*, 2005, **A391**, 221.
- [32] R.Deepak, K.Chichili, T.Ramesh and J.Kevin: *J. Mech. Phys. Solids*, 2004, **52**, 1889.
- [33] M.A.Meyers, G.Subhash, B.K.Kad and L.Prasad: *Mech. Mater.*, 1994, **17**, 175.
- [34] G.A.Li, L.Zhang, C.Ling, R.S.Gao, X.Tan and C.Y.Xu: *Mater. Sci. Eng.*, 2005, **A395**, 81.
- [35] Y.Yan and B.L.Wang: *Mater. Lett.*, 2006, **60**, 2198.
- [36] X.B.Wang, M.Yang, H.J.Yu, L.Hai and Y.S.Pan: *Trans. Nonferrous Met. Soc. China*, 2004, **14**, 335.
- [37] V.F.Nesterenko and M.P.Bondar: *DYMAT J.* 1994, **1**, 245.
- [38] C.Zener and J.H.Hollomon: *J. Appl. Phys.*, 1944, **15**, 22.
- [39] E.M.Trent: *JISI*, 1941, **143**, 401.
- [40] J.H.Andrews, H.Lee and L.Boutne: *JISI*, 1958, **165**, 374.
- [41] D.Scott, B.Loy and G.H.Mills: *Inst. Mech. Eng. Proc.*, 1966-1967, **181**, 20.
- [42] S.C.Liao and J.Duffy: *J. Mech. Phys. Solids*, 1998, **11**, 2201.

- [43] K.A.Hartley, J.Duffy and R.H.Hawley: *J. Mech. Phys. Solids*, 1987, **35**, 283.
- [44] A.Maechan and J.Duffy: *J. Mech. Phys. Solids*, 1988, **36**, 251.
- [45] E.E.Crisman, J.Duffy and Y.C.Chi: *Proc. ASME Symp.on Exp.Tech. in Micromechanics*, ed. W.N.Sharpe, Jr, AMD, **1989**, 163.
- [46] J.Duffy and Y.C.Chi: *Mater. Sci. Eng.*, 1992, **A157**, 195.
- [47] C.O.Mgbokwere, S.R.Nutt and J.Duffy: *Mech. Mater.*, 1994, **17**, 97.
- [48] Y.B.Xu, J.H.Zhang and M.A.Meyers: Research Report on *Shear Localization of Fe-Cr-Ni Monocrystals*, Institute of Metal, Chinese Academy of Sciences, 2005.
- [49] M.G.Mendiratta, A.K.Chakrabarti and J.A.Roberson: *Metall.Trans.*, 1974, **5A**, 1949.
- [50] Dong LI and Xiaojing WAN: *Acta Metall. Sin.*, 1984, **20**, 375. (in Chinese)
- [51] A.K.Zurek: *Metall. Trans.*, 1994, **25A**, 2483.
- [52] Y.B.Xu, L.Liu, J.Q.Yu, L.T.Shen and Y.L.Bai: *Mater. Sci. Technol.*, 2000, **16**, 609.
- [53] Y.B.Xu, W.L.Zhong, Y.J.Chen, L.T.Shen, Q.Liu, Y.L.Bai and M.A.Meyers: *Mater. Sci. Eng.*, 2001, **A299**, 287.
- [54] Q.Li, Y.B.Xu and M.N.Bassim: *J. Mater. Process. Technol.*, 2004, **155**, 1889.
- [55] C.Z.Duan and M.J.Wan: *J. Mater. Sci. Technol.*, 2004, **20**, 775.
- [56] Q.Li: Post-D Research Report, Institute of Metal Research, Chinese Academy of Sciences, 1999.
- [57] B.Dodd and Y.L.Bai: *Mater. Sci. Technol.*, 1989, **5**, 557.
- [58] J.H.Giovanola: *Mech. Mater.*, 1988, **7**, 59.
- [59] G.L.Moss: *Shear Strain, Strain Rates and Temperature Changes in Adiabatic Shear Bands*, eds., M.A.Meyers and L.E.Murr, Shock Waves and High-Strain Rates Phenomena in Metals, Plenum Press, New York, 299.
- [60] R.L.Woodward and R.L.Aghan: *Met. Forum.*, 1979, **1**, 180.
- [61] C.C.Koch, O.B.Cavin, C.G.McKamey and J.O.Scarbrough: *Appl. Phys. Lett.*, 1983, **43**, 1017.
- [62] A.W.Weeber and H.Bakker: *Physica B.*, 1998, **153**, 95.
- [63] M.F.Ashby and R.A.Verrall: *Acta Mater.*, 1973, **21**, 149.
- [64] L.E.Murr, E.A.Trillo, S.Pappu and C.Kennedy: *J. Mater. Sci.*, 2002, **37**, 3337.
- [65] C.M.Glass, G.M.Moss and S.K.Golaski: *Response of Metals to High Velocity Deformation*, eds. P.Shewman and V.F.Zackey, New York, 1961, 115.
- [66] M.C.Mataya, M.J.Carr and G.Krauss: *Metall. Trans.*, 1982, **13A**, 1263.
- [67] Q.Li, Y.B.Xu, Z.H.Lai, Y.L.Bai and L.T.Shen: *J. Mater. Sci. Technol.*, 1999, **15**, 435.
- [68] M.A.Meyers and H.R.Pak: *Acta Mater.*, 1986, **34**, 2493.
- [69] L.E.Murr, C-S.Niou, S.Pappu, J.M.Rivas and S.A.Quinones: *Phys. Status. Solid. A*, 1995, **149**, 253.
- [70] J.A.Hines, K.S.Vecchio and S.Ahzi: *Metal. Trans.*, 1998, **A29**, 191.
- [71] Q.Li, Y.B.Xu, Z.H.Lai, L.T.Shen and Y.L.Bai: *Mater. Sci. Eng.*, 2000, **A276**, 250.
- [72] L.E.Murr, C.S.Niou and C.Feng: *Scripta Metall.*, 1994, **34**, 297.
- [73] V.F.Nesterenko, M.A.Meyers, J.C.LaSalvia, M.P.Bondar, Y.J.Chen and Y.L.Lukyanov: *Mater. Sci. Eng.*, 1997, **A229**, 23.
- [74] Y.B.Xu, Z.Ling, X.Wu and Y.L.Bai: *J. Mater. Sci. Technol.*, 2002, **18**, 504.